Spectrum Splitting Photovoltaics: Polyhedral Specular Reflector Design for Ultra-High Efficiency Modules

Carissa N. Eisler, Emily D. Kosten, Emily C. Warmann, and Harry A. Atwater

California Institute of Technology, Pasadena, CA, 91125, USA

***Abstract* — A design for ultra-high efficiency solar modules (>50%) using spectrum splitting is proposed. In the polyhedral specular reflector design, seven subcells are arranged around a solid parallelepiped. Incident light enters the parallelepiped and is directed via specular reflection onto each subcell in order from highest to lowest bandgap. We analyze optical losses due to external concentration and parasitic absorption and optimize the design for >50% module efficiency. We find that moderate concentration designs (90-170x) with a high index parallelepiped and perfect shortpass filters meet target efficiencies and demonstrate an initial design.**

***Index Terms* — spectrum splitting, multijunction cells**

I. Introduction

In the last decade there has been significant progress in solar cell efficiency, yet ultra-high (>50%) cell and module efficiencies have yet to be achieved [1]. The most realistic approach to achieving ultra-high module efficiencies is via minimization of thermalization losses due to the mismatch between the absorbed photon energy and solar cell bandgap. Multijunction cells address this issue by using multiple subcells, whose materials and bandgaps are chosen as a compromise between minimizing thermalization losses and achieving high device quality (e.g. external radiative efficiency) [2]-[4]. A record efficiency of 44% has recently been achieved [5].

Conventional multijunction solar cells employ monolithic epitaxial fabrication that constrains materials choice to lattice-matched or slightly mismatched lattice parameters and imposed current matching between series-connected subcells interconnected via tunnel junctions. These features can be avoided through the use an external optical component that splits and distributes the solar spectrum to an array of high efficiency subcells that are optically and/or electrically independent. This approach enables multijunction designs using a large number of subcells in which cell design issues are reduced to fabrication of a set of single junction subcells. Various designs for the optical component have been proposed, including holograms [6], light trapping slabs [7], and specular reflection [8]. Here we investigate a polyhedral specular reflector (PSR) design that employs specular reflection to allocate the solar spectrum among subcells. We also evaluate optical losses, show results of ray tracing simulations for initial designs, and describe approaches to increase module efficiency.

II. Polyhedral Specular Reflector Design

In the polyhedral specular reflector (PSR) design, subcells are arranged around a parallelepiped as shown in Figure 1a [9, 10]. Similar to previous designs, incident light enters the parallelepiped shape and is directed onto each subcell from

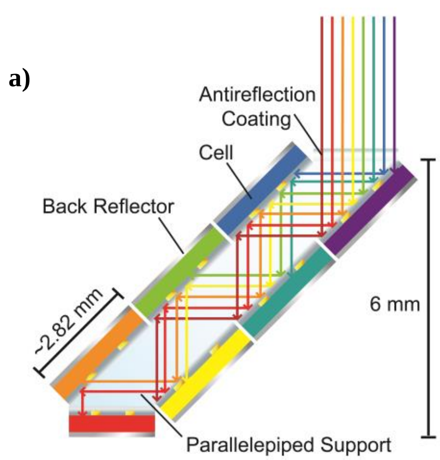

E_g (eV)	III-V Alloy
2.15	$Al_{0.20}Ga_{0.32}In_{0.48}P$
1.84	$Ga_{0.51}In_{0.49}P$
1.58	$Al_{0.1}Ga_{0.9}As$
1.42	GaAs
1.15	$In_{0.87}Ga_{0.13}As_{0.28}P_{0.72}$
0.94	$In_{0.71}Ga_{0.29}As_{0.62}P_{0.38}$
0.74	$In_{0.53}Ga_{0.47}As$

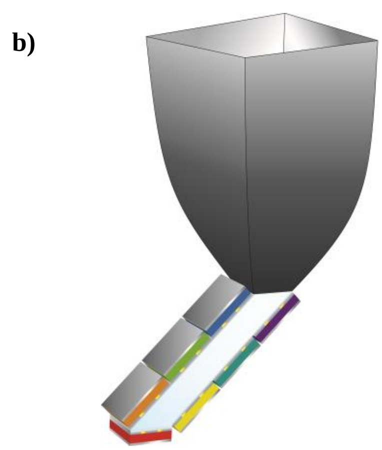

Fig. 1. (a) A schematic of the polyhedral specular reflector with corresponding subcell bandgaps. Cells are mounted on the surface of a solid dielectric parallelepiped and light is specularly reflected through the structure until it is absorbed. The cell thicknesses are not to scale. (b) Schematic of the submodule with a 2-D modified CPC. Height of the CPC is not to scale.

highest to lowest bandgap following a specular optical path within the structure [10]. Thus the lowest energy spectral band is transmitted to the end of the parallelepiped and onto the last subcell. Our design employs shortpass filters to increase reflection efficiency for out-of-band light, which prevents parasitic absorption of sub-bandgap photons via free carrier absorption.

Our design includes seven subcells, as shown in Figure 1, with the seven subcell bandgaps chosen for both optimal matching to the solar spectrum and growth of lattice-matched subcells on GaAs or InP substrates. These bandgaps were chosen by design using detailed balance calculations modified to account for non-ideal cell behavior such as non-radiative recombination and incomplete carrier collection (discussed elsewhere [11]). We assume here that each subcell has an external radiative efficiency (ERE) of 0.3% and 90% of ideal J_{sc}, unless otherwise specified, based on device physics simulations [11]. Additionally, the design incorporates concentration, as shown in Figure 1b, and a solid dielectric parallelepiped support to help accommodate the concentration with fewer optical losses.

III. Exploring Optical Losses: Parasitic Absorption and Reflection at Interfaces

First we explore sources of optical loss inherent in the specular reflection spectrum splitting mechanism: reflection losses between the parallelepiped and cell interfaces and parasitic losses (e.g. free carrier absorption, imperfect back reflectors, etc.) in the subcells. Figure 2a shows the optical efficiency, as a function of the index of refraction of the dielectric parallelepiped and the percentage of parasitic losses in a subcell. Parasitic losses in the subcells dominate the optical efficiency. Reflection losses only misallocate photons to lower bandgap subcells, where they can still be converted, while parasitic absorption prevent the photon from being usefully converted in any subcell. Therefore, to maintain higher than 90% optical efficiency, the parasitic losses in each subcell must remain less than 3-4%. However we estimate from device physics simulations that the parasitic losses due to free carrier absorption to be as high as 10% in each subcell from the doping concentrations and thicknesses of the layers required for high subcell efficiency. To minimize the effects of parasitic absorption, a dielectric filter is mounted between each subcell and the dielectric parallelepiped.

Figure 2b illustrates the performance of a filter designed for the AlGaInP subcell. The filter has high transmission efficiency for the spectral band that the subcell can convert (>2.15 eV) while reflecting most of the lower energy light. This filter was designed for 45° incidence between a glass parallelepiped and a III-V semiconductor using alternating layers of SiO_2 and Ta_2O_5. High filter transmission in the spectral band allocated to each cell is of primary importance to avoid photon absorption in a non-optimal subcell. In addition, lower energy light is reflected, avoiding parasitic absorption. However, the filter presented here has some reflection in the band of interest (<350 nm) and transmission beyond the bandgap (>1325 nm) which will reduce the optical efficiency. Some of these properties are inherent to dielectric multilayer shortpass filter design because of second order reflection bands, making it difficult to produce a filter that is reflective over the entire wavelength range needed. Additionally, the filter properties change significantly for angles other than the specular reflection design angle of 45^{o}, which affects the optical efficiency for light that enters the parallelepiped off normal incidence.

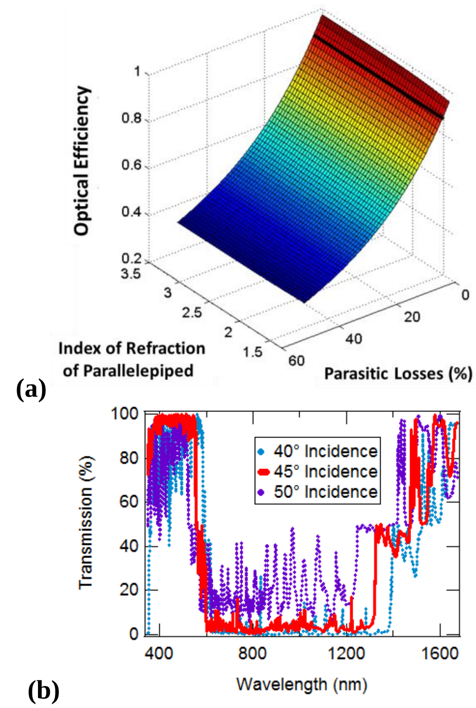

Fig. 2. (a) Optical efficiency as a function of the index of refraction (n) of the parallelepiped structure and parasitic absorptions in the cell. The bold black line denotes 90% optical efficiency. (b) Example filter design for AlInGaP subcell to allow for excellent transmission behavior and prevent parasitic absorption losses.

IV. Incorporating Concentration for >50% Efficiency

The chosen set of seven subcells has an overall detailed balance efficiency of 44.84% under the AM1.5D spectrum at one sun assuming realistic subcell properties (90% of ideal short circuit current (J_{sc}); 0.3% ERE) and no optical losses. Thus optical concentration is needed to exceed 50% module efficiency. However concentration increases the angular spread of light entering the parallelepiped and causes light to stray off of the defined path, where the angular distribution is dictated by refraction upon entering the parallelpiped [11].

$$C = [n_2\sin(\theta_{out})]/[n_1\sin(\theta_{in})]$$

where C is concentration, n_2 and n_1 are the indices of refraction of the parallelepiped and air, respectively, θ_{out} is the spread of angles coming out of the concentrator and θ_{in} is the allowed spread of angles entering the concentrator. Thus a higher concentration requires a larger θ_{out}. A larger angular distribution implies that photons can be misallocated when absorbed by subcells with band gap lower than their target subcell, reducing overall efficiency. This tradeoff is illustrated in Fig. 3, where the optical losses are plotted versus concentration for a two-dimensional trough compound parabolic concentrator on top, oriented such that the spread of angles from the concentrator is in the direction of light splitting [11]. The concentrator has an acceptance angle of 3° and an output angle up to 90°. However we can reduce photon misallocation due to angular spread by using a parallelepiped dielectric material with refractive index n > 1, such as glass or TiO_2. A higher index increases the concentration, as shown by the previous relation, without increasing the angular spread of light. With a higher index parallelepiped, the entering light is refracted closer to the original 45° light path and so the same concentration will have smaller optical losses for a higher index parallelepiped.

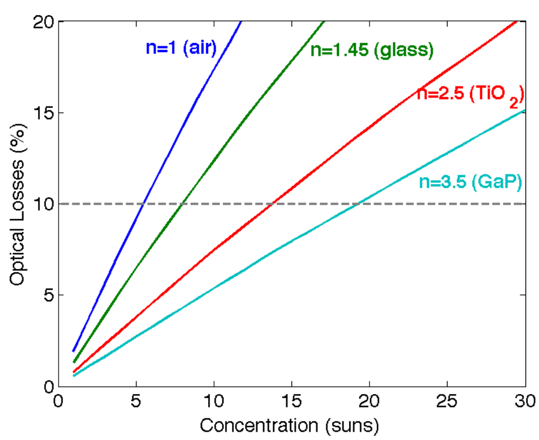

Fig. 3. Optical losses as a function of concentration and parallelepiped-concentrator index of refraction. High concentrations can be achieved with small optical losses when using materials with higher indices of refraction.

To achieve highest efficiencies, the module must balance higher concentration with optical losses by optimizing the design of a three-dimensional compound parabolic concentrator (CPC). The height of the CPC was limited in the design to a maximum of 20 cm, and the output angle was varied which altered the concentration factor. We modeled these concentrators coupled to both fused silica and TiO_2 parallelepipeds, with appropriate shortpass filters using ray tracing simulations. Finally, the spectral band allocated to each subcell was extracted from the simulation and input to the derated detailed balance model to determine the module efficiency for each concentrator design.

Figure 4 shows the variation of module efficiency with concentration as a function of parallelepiped index of refraction and cell performance, for perfect and realistic filters. The perfect filters are assumed to be perfect, omnidirectional shortpass filters with cutoff wavelength equivalent to the bandgap of each subcell. The realistic filter performance was derived from bandpass transmission data for commercially available filters at ideal and nonideal incidence angles. Both types of filters exhibit an efficiency tradeoff: higher higher concentration yields higher subcell voltages but lower system optical efficiency. For perfect filters, it is possible to achieve >50% module efficiency for concentrations between 24 and 90 suns and subcells with an increased carrier collection efficiency (95% of ideal J_{sc}). Even with perfect filters, the efficiency rapidly declines with increasing concentration (>100 suns) because the angular spread becomes high enough to significantly reduce the optical efficiency. This trend is even more pronounced for realistic filters. There is a maximum efficiency of 39.8% (95% ideal J_{sc}) or 37.7% (90% ideal J_{sc}) at 24 suns that is independent of parallelepiped index of refraction. These results indicate that design of filters with improved off-angle performance, relative to the commercial filters evaluated to date, is an important element to enable a PSR design with > 50% efficiency.

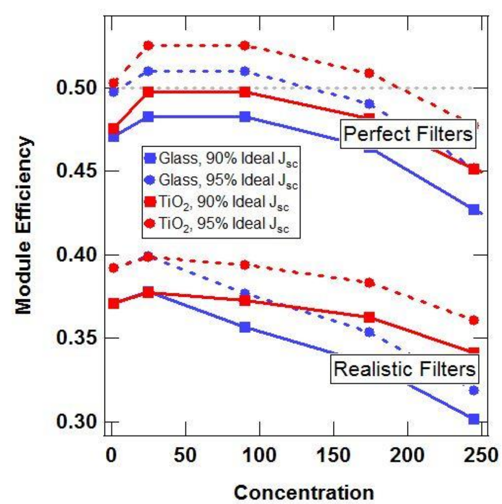

Fig. 4. PSR module efficiency as a function of concentration and parallelepiped index of refraction, for a 3-D CPC with maximum height of 20 cm. 50% efficiency or higher is achieved with high index parallelepipeds and perfect filters. ERE = 0.3% and 90-95% ideal J_{sc} are assumed. Realistic filters exhibit reduced optical and module efficiency.

For commercially available filters, we estimated the variation of module efficiency with ERE and collection efficiency, expressed as a percentage of the ideal J_{sc}. Figure 5 shows the efficiency as a function of these two parameters for a glass parallelepiped under 24x concentration. Significant improvements in module efficiency can be made by improving the current collection or overall material quality. For example, an average ERE of 8% and 90% of ideal J_{sc} will yield 42% module efficiency.

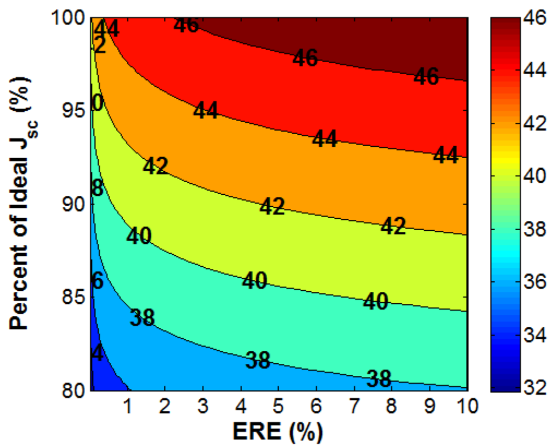

Fig. 5. Contour plot of PSR module efficiency as a function of ERE and % ideal J_{sc} for 24x concentrator and glass parallelepiped design.

V. Future Design Improvements

High optical efficiencies in conjunction with moderate to high concentrations can enable a PSR design with >50% module efficiency. One possible route to improve optical efficiency is the design of less angle-sensitive filters. Another approach is is to reorder the optical sequencing of subcells other than by highest to lowest bandgap. For example, the InGaAs subcell can be positioned first in the light path with an appropriate longpass filter reducing the reflection bandwidth requirement for subsequent shortpass filters. Finally, different concentrator configurations are possible in which concentration is split into two stages with one stage before its designated filter and another concentrator after each filter, enabling higher concentration without a large angular spread (>20°) entering the parallelepiped.

VI. Conclusion

We have developed a spectrum splitting design with potential to achieve greater than 50% module efficiency under the AM1.5D spectrum. For the polyhedral specular reflector, we show that filters are required to prevent parasitic absorption of lower energy light in each subcell, and illustrate an initial filter design. We have also shown the necessity for concentration in the design. Moderate concentration (24-90 suns) yields >50% module efficiency for perfect filters and 37-39% module efficiencies for nonideal, realistic filters. Future work will focus on developing more angularly insensitive filters and improving concentrator designs.

Acknowledgements

This project was supported by the Dow Chemical Company and the DOE 'Light-Material Interactions in Energy Conversion' Energy Frontier Research Center under grant DE-SC0001293. The information, data, or work presented herein was funded in part by the Advanced Research Projects Agency-Energy (ARPA-E), U.S. Department of Energy, under Award Number DE-AR0000333 and the Dow Full Spectrum Project. C. N. Eisler was supported by the by the Department of Defense (DoD) through the National Defense Science & Engineering Graduate Fellowship (NDSEG) Program. The authors wish to thank Sunita Darbe, Michelle Dee, Matthew Escarra, Cris Flowers, Carrie Hofmann, and John Lloyd for helpful discussion and their continued support.

References

[1] Green, M.A., et. al.: 'Solar cell efficiency tables (version 39)', Prog. Photovoltaics, 2012, 20, (1), pp. 12-20

[2] Polman, A., and Atwater, H.A.: 'Photonic design principles for ultrahigh-efficiency photovoltaics', Nat. Mater., 2012, 11, (3), pp. 174-177

[3] Henry, C.H.: 'Limiting Efficiences of Ideal Single and Multiple Energy-Gap Terrestrial Solar-Cells', J. Appl. Phys., 1980, 51, (8), pp. 4494-4500

[4] Marti, A., and Araujo, G.L.: 'Limiting efficiencies for photovoltaic energy conversion in multigap systems', Solar Energy Materials and Solar Cells, 1996, 43, (2), pp. 203-222.

[5] Wiemer, M., et. al.: '43.5% efficient lattice matched solar cells.' Proc. of SPIE, 2011, 8108, pp. 810804-810804.

[6] Escarra, M.D., et. al.: 'Spectrum-Splitting Photovoltaics: Holographic Spectrum Splitting in Eight-Junction, Ultra-high Efficiency Module' PVSC, 2013, (accepted).

[7] Kosten, E.D., et. al.: 'Spectral Splitting via a Light Trapping Filtered Concentrator for Ultrahigh Photovoltaic Efficiency' PVSC, 2013, (accepted).

[8] Imenes, A.G., and Mills, D.R.: 'Spectral beam splitting technology for increased conversion efficiency in solar concentrating systems: a review', Solar Energy Materials and Solar Cells, 2004, 84, (1-4), pp. 19-69

[9] Ellion, M., Edmund: 'High Efficiency Photovoltaic Assembly'. World Patent 8,701,5121987

[10] Mitchell, B., et. al.: 'Four-junction spectral beam-splitting photovoltaic receiver with high optical efficiency', Progress in Photovoltaics, 2011, 19, (1), pp. 61-72

[11] Warmann, E.C., et. al.: 'Proposed Band gaps and Materials for Spectral Splitting Photovoltaics to Achieve 50% System Efficiency' PVSC, 2013, (accepted).

[12] Escarra, M., et. al.: 'III-V Photovoltaics for Full Spectrum Ultrahigh Efficiency Solar Energy Conversion' Spring MRS, 2013, (accepted).

[13] Green, M.A.: 'Radiative efficiency of state-of-the-art photovoltaic cells', Progress in Photovoltaics: Research and Applications, 2012, 20, (4), pp. 472-476

[14] Welford, W.T., and Winston, R.: 'High Collection Nonimaging Optics' (Academic Press, Inc., 1989. 1989).